AD-A099 388 NAVAL RESEARCH LAB WASHINGTON DC F/G 4/1
DIFFUSION OF SMALL-SCALE DENSITY IRREGULARITIES DURING EQUATORI--ETC(U)
MAY 81 J D HUBA, S L OSSAKOW
UNCLASSIFIED NRL-MR-4521 NL

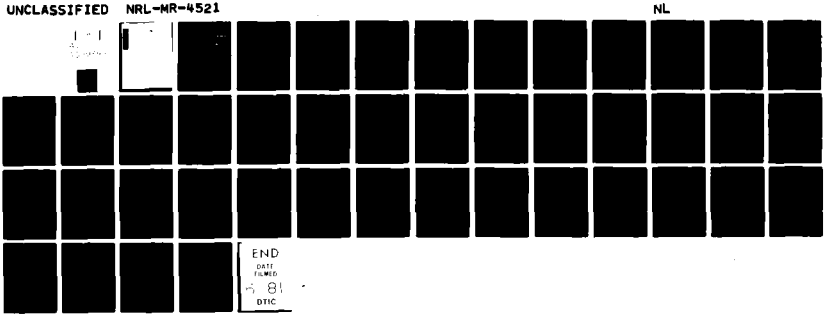

SECURITY CLASSIFICATION OF THIS PAGE (When Data Entered)

REPORT DOCUMENTATION PAGE	READ INSTRUCTIONS BEFORE COMPLETING FORM
1. REPORT NUMBER: NRL Memorandum Report 4521	2. GOVT ACCESSION NO.: AD-A099 388
3. RECIPIENT'S CATALOG NUMBER	
4. TITLE (and Subtitle): DIFFUSION OF SMALL-SCALE DENSITY IRREGULARITIES DURING EQUATORIAL SPREAD F	5. TYPE OF REPORT & PERIOD COVERED: Interim report on a continuing NRL problem.
6. PERFORMING ORG. REPORT NUMBER: NRL-MR-4521	
7. AUTHOR(s): J. D. Huba* S. L. Ossakow	8. CONTRACT OR GRANT NUMBER(s): RR03302, S990AXH; RR033024, C0926
9. PERFORMING ORGANIZATION NAME AND ADDRESS: Naval Research Laboratory, Washington, D.C. 20375	10. PROGRAM ELEMENT, PROJECT, TASK AREA & WORK UNIT NUMBERS: 61153N; RR0330244; 47-0883-0-1; 62704H; 47-0889-0-1
11. CONTROLLING OFFICE NAME AND ADDRESS: Defense Nuclear Agency, Washington, D.C. 20305; Office of Naval Research, Arlington, VA 22217	12. REPORT DATE: 28 May 1981
	13. NUMBER OF PAGES: 44
14. MONITORING AGENCY NAME & ADDRESS (if different from Controlling Office)	15. SECURITY CLASS. (of this report): UNCLASSIFIED
	15a. DECLASSIFICATION/DOWNGRADING SCHEDULE

16. DISTRIBUTION STATEMENT (of this Report)

Approved for public release; distribution unlimited.

DTIC ELECTE MAY 27 1981 S D C

17. DISTRIBUTION STATEMENT (of the abstract entered in Block 20, if different from Report)

18. SUPPLEMENTARY NOTES

*Science Applications, Inc., McLean, VA 22102. Present address: Geophysical and Plasma Dynamics Branch, Plasma Physics Division, Naval Research Laboratory, Washington, D.C. 20375.

(Continues)

19. KEY WORDS (Continue on reverse side if necessary and identify by block number)

Diffusive decay
Small scale density irregularities
Equatorial spread F
Anomalous diffusion
Time scales

20. ABSTRACT (Continue on reverse side if necessary and identify by block number)

The diffusion of small-scale density irregularities (i.e., those with density gradient scale lengths less than several hundred meters) is investigated during the decay phase of equatorial spread F. Both classical and anomalous diffusion processes are considered. The anomalous diffusion coefficient is based upon the transport properties associated with the universal drift instability. It is found that anomalous diffusion can smooth out small-scale density irregularities on time scales, τ, consistent with observational results, i.e.,

(Continues)

DD FORM 1 JAN 73 1473 EDITION OF 1 NOV 65 IS OBSOLETE
S/N 0102-014-6601

SECURITY CLASSIFICATION OF THIS PAGE (When Data Entered)

18. Supplementary Notes (Continued)

This research was sponsored partially by the Defense Nuclear Agency under Subtask S99QAXHC, work unit 00002, work unit title, "Plasma Structure Evolution," and partially by the Office of Naval Research.

20. Abstract (Continued)

few minutes $\lesssim \tau \lesssim$ few hours. On the other hand, classical diffusion is much too slow a process to be important. However, anomalous diffusion is unable to diffuse large-scale irregularities, i.e., those with scale lengths greater than a kilometer, on the time scales $\tau \lesssim$ few hours and another mechanism must occur to smooth out these irregularities, e.g., shorting out to the E region.

tau L or a, approx. =

approx. = tau L or approx. =

CONTENTS

DIFFUSION OF SMALL-SCALE DENSITY IRREGULARITIES DURING EQUATORIAL SPREAD F

I. INTRODUCTION

Over the past few years a considerable amount of effort has been directed at understanding the physical processes associated with equatorial spread F. Major advances have been made both experimentally (Kelley et al., 1976; Woodman and La Hoz, 1976; McClure et al., 1977; Huba et al., 1978; Weber et al., 1978; Tsunoda and Towle, 1979; Towle, 1980; Tsunoda, 1980, Szuszczewicz et al., 1980; Tsunoda, 1981; Rino et al., 1981; Keskinen et al., 1981) and theoretically (Haerendel, 1974; Hudson and Kennel, 1975; Scannapieco and Ossakow, 1976; Chaturvedi and Ossakow, 1977; Ott, 1978; Ossakow and Chaturvedi, 1978; Costa and Kelley, 1978a,b; Huba et al., 1978; Ossakow et al., 1979; Keskinen et al., 1980; Zalesak and Ossakow, 1980; Sperling and Goldman, 1980; Keskinen et al., 1981; Huba and Ossakow, 1981a,b; for a complete review through 1980, see Ossakow, 1981) in this area. Presently, much of the research on spread F is focussed on small-scale irregularities; that is density fluctuations occurring on scale lengths less than several hundred meters. A brief overview of this work is as follows.

The first indication of small-scale density fluctuations being present during equational spread F is the 3 m backscatter radar measurements made at Jicamarca in the early seventies (Farley et al., 1970). Since the mean ion gyro-radius is ~ 4 m, these observations show that turbulence exists on scale lengths smaller than the ion gyro-radius. Moreover, power spectral density and radar backscatter measurements (Woodman and Basu, 1978)

Manuscript submitted March 25, 1980.

suggest that the actual observed 3 m radar backscatter power is substantially below (3-4 orders of magnitude) the extrapolated in situ k^{-2} spectrum from longer wavelengths (i.e., $\gtrsim$100 m). Thus, the 3 m irregularities do not appear to be caused by a turbulent cascade of energy from smaller wave numbers. Recently, backscatter measurements have been made using the ALTAIR (Kuba et al., 1978; Towle, 1980; Tsunoda and Towle, 1979; Tsunoda, 1981) and TRADEX (Tsunoda, 1980) radar systems at Kwajalein and have found fluctuations at 1 m, 36 cm, and 11 cm. It appears then that turbulence even exists at wavelengths comparable to the mean electron gyro-radius (~3 cm).

In situ satellite (McClure et al., 1977) and rocket (Kelley et al., 1976; Morse et al., 1977; Szuszczewicz et al., 1980) experiments have also been performed during equatorial spread F. The major result relevant to the small-scale irregularities is the observation of steep plasma density gradients (Costa and Kelley, 1978a; Kelley et al., 1981; Szuszczewicz, private communication, 1980). These sharp density gradients presumably arise from the nonlinear development of plasma macroinstabilities (e.g., Rayleigh-Taylor). Density gradient scale lengths have been observed as small as 30 m, although typically they are $\gtrsim$75 m. Also, correlative studies indicate that the strongest radar backscatter signals coincide with the walls of plasma bubbles, i.e., regions of steep density gradients (Szuszczewicz et al., 1980; Tsunoda, 1981). Based on these observations, the most plausible explanation for the small-scale irregularities is the excitation of drift waves. In the wavelength regime $kr_{Li} \lesssim 1$ (r_{Li} is the near ion gyro-radius), which corresponds to scale-sizes greater

than 25 m, the universal drift (collisionless; Costa and Kelley, 1978a,b), or drift dissipative (collisional; Goldman and Sperling, 1980; Huba and Ossakow, 1979a) instabilities may be operative depending upon the physical parameters (e.g., collision freguencies). However, at wavelengths corresponding to the 3 m irregularities, ion viscuous damping prevents the linear excitation of these instabilities for typical spread F conditions (Huba and Ossakow, 1979a). It has been suggested that these irregularities may be generated via a parametric process driven by a large-amplitude, long wavelength mode (Huba and Ossakow, 1979a). On the other hand, the generation of the 1 m, 36 cm and 11 cm irregularities are probably due to the lower-hybrid-drift instability (or possibly the drift cyclotron instability) which exists in the regime $kr_{Le} \lesssim 1$, where r_{Le} is the mean electron gyro-radius (Huba et al., 1978; Huba and Ossakow, 1979b; Huba and Ossakow, 1981a,b)

A question naturally arises: what is the influence of the drift wave turbulence on the evolution of the plasma? Laboratory experiments indicate that the dominant effect is anomalous diffusion of plasma across the magnetic field to smooth out density gradients. That is, particles interact with the collective electric fields associated with the instability and are able to scatter across field lines. Thus, in general, drift instabilities act to destroy the free energy source which drive them, i.e., the density gradients. Of course, the ionospheric F region is not collisionless and the classical electron-ion collision frequency can be significant (i.e., $\nu_{c\ell} / \Omega_i \sim 1\text{-}5$ where $\nu_{c\ell}$ is the classical

electron-ion frequency and Ω_i is the ion gyro-frequency) depending on the value of the density. Coulomb collisions may also be important in the cross-field diffusion of plasma. Collisions with neutral particles also occur but are less frequent than electron-ion collisions at altitudes above 300 km.

Observationally, diffusion appears to be the dominant mechanism which smooths out the steep density gradients; those such that $L_n \lesssim$ several hundred meters where L_n is the density gradient scale length. By this we mean the following. In the hierarchy of small-scale irregularities responsible for the radar backscatter measurements, the smaller the irregularity size, the steeper the density gradient scale length required to support it. Very sharp density gradients ($L_n \lesssim 100$ m) are necessary to excite the lower-hybrid-drift instability which is responsible for the 1 m, 36 cm, and 11 cm irregularities. On the other hand, weaker density gradients ($L_n \gtrsim 100$ m) can drive the longer wavelengths modes ($kr_{Li} \lesssim 1$) which are probably necessary to generate the 3 m irregularities. Since the time scale associated with a diffusion process is $\tau_D \sim \lambda^2/D$ (λ is a scale length and D is the diffusion coefficient), the shortest density gradient scale lengths diffuse away first. Thus, one would expect the smallest scale irregularities to disappear first in the decay phase of equatorial spread F and this, in fact, seems to be the case (Basu et al., 1978; Basu et al., 1980).

The purpose of this paper is to examine both clsasical and anomalous diffusion processes for equatorial spread F conditions. As such, we will neglect all driving forces, which generate

equatorial spread F irregularitites, and consider the pure diffusive decay of such irregularities. We focus on the steeper density gradient scale lengths (i.e., $L_n \lesssim$ several hundred meters), since diffusion is much too slow to be important in the evolution of the large-scale irregularities ($L_n \gtrsim 1$ km). Our main conclusion is that anomalous diffusion is the dominant diffusion mechanism for spread F.

The scheme of the paper is as follows. In the next section we present the diffusion equation and a discussion of the diffusion coefficients considered. For the anomalous diffusion coefficient we base our analysis on the universal drift instability. In Section III we discuss this choice of the anomalous diffusion coefficient. Section IV contains the results of a numerical analysis of the diffusion equation for both classical and anomalous diffusion coefficients. In the final section we apply our results to equatorial spread F. We also present similarity solutions to the diffusion equation in the Appendix.

II THEORY

We consider the problem of cross-field diffusion of plasma in a low β plasma ($\beta<<1$, where $\beta=8\pi n(T_e+T_i/B^2)$). The one-dimensional diffusion equation can be written as

$$\frac{\partial n}{\partial t} = \frac{\partial}{\partial x}\left(D \frac{\partial n}{\partial x}\right) \tag{1}$$

where [Perkins et al., 1973]

$$D = \nu_{ei} \frac{\beta}{2} \frac{c^2}{\omega_{pe}^2} \tag{2}$$

ν_{ei} is the electron-ion collision frequency (either classical or anomalous) and $\omega_{pe} = (4\pi ne^2/m_e)^{\frac{1}{2}}$ is the electron plasma frequency. Note that we assume a one-dimensional slab geometry which is adequate for small-scale spread F irregularities. The one dimensionality simplifies the analysis, of course, but it is a reasonable assumption given that the irregularities during ESF are generated by steep gradients, e.g., the walls of bubbles. Also, we assume $T_e = T_i$ and have neglected electron-neutral collisions.

We choose the following collision frequencies for our analysis:

$$\text{Classical:} \quad \nu_{ei} = \nu_{c\ell} = (\lambda_c/3.5 \times 10^5)(n_e/T_e^{3/2}) \text{ sec}^{-1} \tag{3}$$

$$\text{Anomalous:} \quad \nu_{ei} = \nu_{an} = (2\pi/9)\,|\epsilon_n\, r_{Li}|\,\Omega_e \tag{4}$$

In Equations (3) and (4) λ_c is the Coulomb logarithm ($\lambda_c = 23.4 - 1.15 \log n_e + 3.45 \log T_e$), $\epsilon_n = |d\,\ell n\, n/d_x|^{-1} = 1/L_n$ where L_n is the density gradient scale length, r_{Li} is the mean ion gyro-radius, Ω_e is the electron gyro-frequency, n_e is in cm^{-3} and T_e is in eV. The anomalous collision frequency used is based upon the anomalous transport properties associated with the universal drift instability (Gary, 1980). We discuss this choice shortly. These collision frequencies lead to the following diffusion coefficients:

$$\text{Classical:} \quad D = D_{c\ell} = \nu_{c\ell}^{o} \rho_{es}^2 \, (n/n_o) \tag{5}$$

$$\text{Anomalous:} \quad D = D_{an} = \frac{4\pi}{9} |\varepsilon_n \, r_{Li}| \rho_{es}^2 \, \Omega_e \tag{6}$$

where $\rho_{es} = \left[(T_e/T_i)/m_e\right]^{1/2}/\Omega_e$ is an effective electron gyroradius, n_o is a normalization density and $\nu_{c\ell}^{o} = \nu_{c\ell}(n_e=n_o)$. From Eqs.(5)-(7) it is evident that

$$\frac{D_{c\ell}}{D_{an}} \sim \frac{\nu_{c\ell}^{o}}{\Omega_e} \, |\varepsilon_n \, r_{Li}|^{-1} \tag{7}$$

Thus, for typical spread F conditions it is found that $D_{c\ell} << D_{an}$ and one expects anomalous diffusion to dominate over classical diffusion.

We finally substitute Eqs. (5)-(7) into Eq. (1) and arrive at the following diffusion equations:

$$\text{Classical:} \quad \frac{\partial n}{\partial t} = \nu_{c\ell}^{o} \rho_{es}^2 \, \frac{\partial}{\partial x} \left(\frac{n}{n_o} \, \frac{\partial n}{\partial x} \right) \tag{8}$$

$$\text{Anomalous:} \quad \frac{\partial n}{\partial t} = \frac{4\pi}{9} \Omega_e \rho_{es}^2 \, \frac{\partial}{\partial x} \left(|\varepsilon_n \, r_{Li}| \, \frac{\partial n}{\partial x} \right) \tag{9}$$

We now transform to dimensionless variables and obtain

$$\text{Classical:} \quad \frac{\partial \tilde{n}}{\partial \tau_{c\ell}} = \frac{\partial}{\partial s} \left(\tilde{n} \, \frac{\partial \tilde{n}}{\partial s} \right) \tag{10}$$

$$\tilde{n} = n/n_o; \quad s = x/\lambda; \quad \tau_{c\ell} = (\rho_{es}^2/\lambda^2)\,(\nu_{c\ell}^o)$$

$$\text{Anomalous: } \frac{\partial \tilde{n}}{\partial \tau_{an}} = \frac{\partial}{\partial s}\left(\left| \frac{1}{\tilde{n}} \frac{\partial \tilde{n}}{\partial s} \right| \frac{\partial \tilde{n}}{\partial s} \right) \tag{11}$$

$$\tilde{n} = n/n_o; \quad s = x/\lambda; \quad \tau_{an} = \frac{4\pi}{9} \frac{\rho_{es}^2}{\lambda^2} \frac{r_{Li}}{\lambda} \quad (\Omega_e t)$$

Clearly, Eqs. (10) and (11) are non-linear partial differential equations. We solve them numerically as initial value problems in Section IV. They also possess similarity solutions which offer some insight into the scaling of diffusion process. We discuss these solutions in the Appendix. However, we now discuss our choice of the anomalous diffusion coefficient.

III. ANOMALOUS DIFFUSION

As mentioned earlier, the collective electric fields associated with a plasma instability driven by a density gradient can cause particles to be scattered across magnetic field lines, which leads to anomalous diffusion of plasma. This process can eventually smooth out the density gradient and suppress the instability. Several estimates of the anomalous diffusion coefficient for this phenomenon have been given based upon a variety of physical arguments. Perhaps the best known is

$$D_{an} \lesssim \gamma/k_\perp^2 \tag{12}$$

which is derived heuristically by Kadomtsev (1965) for a strongly turbulent plasma (i.e., $\gamma \sim \omega_r$ where $\omega = \omega_r + i\gamma$). More sophisticated derivations of this relationship have been presented although there are criticisms of this estimate.

Nevertheless, Eq. (12) is used frequently, primarily because of its simplicity.

An alternative procedure to estimate the anomalous diffusion coefficient is based upon quasi-linear theory. Second-order Vlasov theory is used to define an anomalous collision frequency which can then be determined from the linear properties of the mode and the saturation energy of the instability. The diffusion coefficient is then found from Eq. (2).

In this paper we opt for the second approach and base our analysis on the universal drift instability, i.e., collisionless drift instability. (It should be noted that Kelley et al., 1981, have suggested that collisionless drift mode waves are the most likely candidate for the observed electric field and density fluctuation spectra in the 10-100 m regime). The details of this method are outlined by Gary (1980) and we do not reproduce them here. However, several comments should be made. First, the estimate of D_{an} given by Eq. (7) is, in fact, comparable to that of Eq. (12). Second, Eq. (7) explicitly contains the density gradient which is consistent with the notion that diffusion occurs in regions that are unstable. This dependence on L_n leads to the nonlinearity of the diffusion equation. Finally, other instabilities, such as the drift dissipative (collisional drift instability) (Goldman and Sperling, 1979) or the lower-hybrid-drift instability, could also be relevant. Whether the universal drift instability is excited depends upon the classical electron-ion collision frequency $\nu_{c\ell}$, which, in turn, depends

upon the density. Typically, $\nu_{c\ell}/\Omega_i \sim 0.8\text{-}5$ for electron density in the range $10^4 - 10^6$ cm^{-3}. For unstable modes in the regime $kr_{Li} \lesssim 1$ it is found that the drift instability is neither purely collisionless, nor purely collisional (Huba and Ossakow, 1979a). Also estimates of the diffusion coefficient associated with the drift dissipative instability are comparable to that of the universal drift instability (Kadomtsev, 1965). Thus, although collisions affect the universal drift instability for typical spread F conditions, use of the anomalous diffusion coefficient associated with this mode is justified since it is qualitatively accurate (i.e., $D \propto L_n^{-1}$) and is quantitatively accurate to within a factor of 2 or 3. On the other hand, the anomalous diffusion coefficient of the lower-hybrid-drift instability is substantially smaller than that of the universal drift instability and can be neglected (Gary, 1980).

IV. NUMERICAL RESULTS

We solve Eqs. (10) and (11) numerically as an initial value problem using a leap-frog scheme for the temporal variation and a fourth-order, finite difference scheme for the spatial variation. We choose as the initial density profile

$$\tilde{n}\ (s,\ \tau=0) = (1-\varepsilon)^{-1}\ [1 + \varepsilon\ \tanh s] \qquad (13)$$

where $0 \leq \varepsilon < 1$, $s = x/\lambda$, and $\tilde{n} = n(s)/n(s=-\infty)$. Here, ε determines the magnitude of the density change across the boundary layer λ. The boundary condition is $\partial n/\partial s = 0$ at the boundaries (i.e., $|s| >> 1$) and $n(|s| \rightarrow \infty, \tau) = n(|s| \rightarrow \infty, 0)$. We choose Δt

sufficiently small so that the Courant-Levy condition is satisfied to prevent numerical instability. The grid size Δs is varied to insure that an asymptotic solution is obtained as $\Delta s \to 0$. For the results presented below we choose $\varepsilon = 0.9$ so that the density changes approximately an order of magnitude across the boundary layer λ. For different values of ε, the results remain qualitatively the same although quantitative changes occur. We also point out that λ is a constant which characterizes the initial width of the boundary layer. However, λ is not the same as the scale length of the density gradient L_n. The density gradient scale length is defined by $L_n = \lambda \left[d \ell n \, n/ds \right]^{-1}$ and varies across the boundary layer. It is the density gradient scale length L_n that is critical to the excitation of drift instabilities and not λ.

A. Classical Diffusion

We expand Eq. (10) to obtain

$$\frac{\partial \tilde{n}}{\partial \tau_{c\ell}} = \left(\frac{\partial \tilde{n}}{\partial s} \right)^2 + \tilde{n} \frac{\partial^2 \tilde{n}}{\partial s^2} \tag{14}$$

where $\tau_{c\ell} = \nu_{c\ell}^{o} t \, (\rho_{es}^2/\lambda^2)$. The solution to this equation is shown in Figure 1 which plots $\tilde{n}(s,\tau)$ vs. s at times $\tau_{c\ell} = 0.0$, 0.2, and 0.4. As is expected, the width of the boundary layer is increasing with time. Note that diffusion is occurring more rapidly in the region $s>0$ than the region $s<0$. This occurs because of the density dependence of the diffusion coefficient.

Since $D_{c\ell} \propto n$ and the density is greater for $s>0$ than $s<0$, the diffusion coefficient is larger for $s>0$ and faster diffusion takes place in this region.

In figures 2a and 2b, we plot the spatial and temporal variation of the inverse density gradient scale length. In Figures 2a we show λ/L_n vs. s(where $\lambda/L_n = (1/\tilde{n})\ \partial\tilde{n}/\partial s$) for $\tau_{c\ell} = 0.0$, 0.2 and 0.4. The shortest density gradient scale lengths exist in the region $s<0$ due to the $(1/\tilde{n})$ dependence of L_n^{-1}. However, it is interesting to note that the maximum inverse gradient scale length actually <u>increases</u> during the initial evolution of the density profile. This is better shown in figure 2b, which plots $(\lambda/L_n)_{max}$ vs. $\tau_{c\ell}$. The inverse gradient scale length increases $\sim$20% in a time $\tau_{c\ell} \sim 0.06$. After this time it decreases monotonically.

The reason for the initial steepening of the density profile can be understood as follows. From Eq. (14) we find that

$$\tilde{n}(s,\tau+\Delta\tau) \sim \tilde{n}(s,\tau) + \Delta\tau \left[(\partial\tilde{n}/\partial s)^2 + \tilde{n}\ \partial^2\tilde{n}/\partial s^2\right] \qquad (15)$$

for $\Delta\tau<<\tau$. A portion of the initial profile $\tilde{n}(s,\tau)$ is shown in Figure 3 by the solid line (not drawn to scale), and we have isolated 3 points (s_0, s_1, s_2). Note that $(\partial\tilde{n}/\partial s)^2 > 0$ and $(\partial^2\tilde{n}/\partial s^2) > 0$ for the region shown so that both terms in the brackets of Eq. (15) initially tend to increase the density for $s_0<s<s_2$. At $s=s_1$ the density increases an amount $\Delta\tilde{n}_1$ and at $s=s_2$ the density increases amount $\Delta\tilde{n}_1$, in a time $\Delta\tau$. However, $\Delta\tilde{n}_2>\Delta\tilde{n}_1$ since $(\partial\tilde{n}/\partial s)_{s_2}>(\partial\tilde{n}/\partial s)_{s_1}$, and $\tilde{n}_2>\tilde{n}_1$. This can be shown easily if we take $\tilde{n}\sim\tilde{s}^2$ in the region $s_0<s<s_2$.

Physically, since D∝n, the diffusion coefficient is larger at s_2 than s_1 and more particles diffuse to s_2 from $s>s_2$ than to s_1 from $s>s_1$. Thus, a steepening of the density profile occurs. This process continues until $\partial^2\tilde{n}/\partial s^2 \lesssim 0$ at $s=s_2$ so that $\Delta\tilde{n}_1 > \Delta\tilde{n}_2$. This can be seen by noting the evolution of $\tilde{n}$ and (λ/L_n) at $s=s_1$ in Figures 1 and 2a. At $\tau = 0.2$ the density profile has steepened (i.e., λ/L_n has increased from its value at $\tau = 0.0$) and $\partial^2\tilde{n}/\partial s^2>0$. However, at $\tau = 0.4$ the profile has become less steep (i.e., λ/L_n has decreased from its value at $\tau = 0.2$) and $\partial^2 n/\partial s^2 < 0$.

B. Anomalous Diffusion

We rewrite Eq. (11) as

$$\frac{\partial \tilde{n}}{\partial \tau_{an}} = \left|\frac{1}{\tilde{n}} \frac{\partial \tilde{n}}{\partial s}\right| \left[-\frac{1}{\tilde{n}}\left(\frac{\partial \tilde{n}}{\partial s}\right)^2 + 2\frac{\partial^2 \tilde{n}}{\partial s^2}\right] \qquad (16)$$

where $\tau_{an} = (4\pi/9)(\rho_{es}^2/\lambda^2)(r_{Li}/\lambda)\,\Omega_e t$. Note the explicit dependence on λ/L_n so that diffusion only occurs in regions of the plasma density gradient (i.e., only the regions which can support drift waves). The temporal evolution of the initial profile $n(s,\tau=0)$ is shown in Figure 4 for times τ_{an}=0.0, 1.0, and 2.0. In contrast to the classical diffusion process, the largest amount of diffusion is occurring in the region $s<0$. This is simply due to the fact that D_{an} is largest in this region. The spatial and temporal evolutions of (λ/L_n) are shown in Figures 5a and 5b. In Figure 5a, it is clear that (λ/L_n) is more pervasive for $s<0$ than $s>0$. Also the maximum inverse gradient

scale length is decreasing in time. This is shown in Figure 5b, which indicates that $(\lambda/L_n)_{max}$ decreases monotonically in time and has decreased by $\geq 50\%$ during the time period considered. This result is consistent with the notion that the effect of the drift instability is to smooth out the plasma density gradient.

V. APPLICATION TO EQUATORIAL SPREAD F

It has been shown that both classical and anomalous diffusion processes tend to smooth out density gradients. The question remains as to which process dominates during equatorial spread F. The key parameter which can answer this question is the time scale of each process. In Table I we contrast the classical and anomalous diffusion time scales for parameters typical of equatorial spread F. We remind the reader that

$$\text{Classical:} \quad t_{c\ell} = (\lambda^2/\rho_{es}^2)\, \tau_{c\ell}/\nu_{c\ell}^o \tag{17}$$

$$\text{Anomalous:} \quad t_{an} = (9/4\pi)\, (\lambda^2/\rho_{es}^2)\, (\lambda/r_{Li})\, \tau_{an}/\Omega_e \tag{18}$$

where $\nu_{c\ell}^o = \nu_{c\ell}\,(n(s=-\infty))$, $\rho_{es}^2 = (T_e+T_i)/m_e\Omega_e^2$, $r_{Li} = (T_i/m_i)^{\frac{1}{2}}/\Omega_i$, $\Omega_e = eB_o/m_e c$ and λ is the initial scale length. We choose $T_e = T_i = 0.1$ eV, $B = 0.3$ G, $n(s=-\infty)=10^5$ cm^{-3} and consider an 0^+ plasma. For these parameters we find that $\rho_{es} = 3.5$ cm, $r_{Li} = 4.3$ m, $\nu_{c\ell}^o = 130$ sec^{-1} and $\Omega_e = 5.3 \times 10^6$ sec^{-1}. The time scales Eqs. (17) and (18) are shown in Table I for several initial scale lengths, $\lambda = 50$ m, 100 m, 200 m, and 500 m. The

corresponding minimum initial density gradient scale lengths are L_n=40 m, 80 m, 160 m, and 400 m where $L_n=(d\ell n n/dx)^{-1}$. It should be noted immediately from Table I that the time scale for the classical diffusion process is hours while that for the anomalous diffusion process is minutes. As anticipated from Eq. (7), classical diffusion is a much slower process than anomalous diffusion for the F region ionospheric plasma. Moreover, since the initial tendency of classical diffusion is to steepen the density profile, at least an hour passes before the density gradient begins to weaken for the situation in Table I. On the other hand, the action of the anomalous diffusion process is to always smooth out the density gradient. For initially steep gradients ($L_n \lesssim 100$ m), wave turbulence can double their scale lengths in several minutes ($t \lesssim 5$ min). However, several hours are needed to diffuse density profiles to scale lengths on the order of a kilometer. In order to significantly diffuse density gradient scale lengths greater than a kilometer, many hours are required ($\gtrsim$8 hrs.) since $t_{an} \propto \lambda^3$.

There is experimental evidence that suggests steep density gradients ($L_n \lesssim 100$ m) relax in a time $\lesssim 5$ minutes. Szuszczewicz et al.(1980) has observed intense 1 m backscatter from the ALTAIR radar at Kwajalein during the decay phase of equatorial spread F. The most intense backscatter signal appears to decay away on the time scale $\lesssim 5$ minutes. Presumably, very sharp density gradients exist to produce the 1 m density fluctuations via lower-hybrid-drift instability ($L_n \lesssim 100$ m). Since anomalous diffusion can smooth out the sharp density gradients on this time scale, then it is

likely that the lower-hybrid-drift mode is also suppressed on this time scale. This would cause the 1 m backscatter signals to weaken considerably, consistent with observations. Also, as indicated earlier, in the decay phase of equatorial spread F, the smallest density irregularity scale-sizes disappear first, (Basu et al., 1978; Basu, 1980), i.e., 36 cm backscatter fades before the 1 m backscatter, the 1 m backscatter fades before the 3 m backscatter, and so on, which is also consistent with an anomalous diffusion process due to drift waves since $t_{an} \propto \lambda^3$. On the other hand, large scale density irregularities ($L_n \gtrsim 1$ km) are observed to decay in several hours (Basu et al., 1980; Aarons et al., 1980) and this process cannot be explained by diffusion, even anomalous diffusion.

VI. CONCLUSION

The purpose of this paper is to examine the diffusion of density irregularities during equatorial spread F. We have considered both classical and anomalous diffusion processes. A major assumption in our analysis is that any driving mechanism which produces the density irregularities ($L_n \lesssim$ several hundred meters) has ceased. Presumably the small-scale irregularities are generated nonlinearly from a macroinstability (e.g., Rayleigh-Taylor). Thus, we limit our attention to the decay phase of equatorial spread F.

Experimentally, diffusion seems to be the dominant process which smooths out sharp density gradients ($L_n \lesssim$ several hundred meters). This is based on the fact that the diffusion time is

proportional to some power of the diffusion length [Eqs. (17) and (18)]. Thus, the shorter density gradient scale lengths diffuse away before the longer ones. Observationally this is suggested by the order of the decay of radar backscatter signals (i.e., the shortest ones fade away first) which are due to drift wave turbulence. Also the time scale associated with this process is of the order of minutes.

Based on our analysis, we find that an anomalous diffusion process is consistent with these observations while classical diffusion is much too slow. The anomalous diffusion is based upon drift wave turbulence presumed to exist at wavelengths such that $kr_{Li} \sim 1$. We have considered an explicit model for the anomalous diffusion coefficient based upon the collisionless universal drift instability. Although collisions probably modify the dispersive properties of the mode, the anomalous diffusion coefficient is not expected to be significantly different (neither qualitatively nor quantitatively). On the other hand, diffusion of large scale irregularities ($\lambda \gtrsim 1$ km) does not seem possible since the time scale associated with this process is many hours ($\gtrsim 8$ hrs.). Another mechanism must occur to smooth out these irregularities, e.g., shorting out to the E region (which continuously builds up in the morning hours).

A possible scenario is that anomalous diffusion causes the gradient scale lengths $L_n \lesssim$ several hundred meters, which drive the radar backscatter observed irregularities ($\lesssim 3$ m), to disappear on time scales of the order of minutes. Radar backscatter observed irregularities ($\lesssim 3$ m), themselves without the driving

gradient scale lengths, can disappear by either classical or anomalous diffusion. Scintillation causing irregularities (> 1 km) cannot decay by either classical or anomalous diffusion because it requires too much time (> 8 hrs.). However, these long wavelengths can couple effectively via the high conductivity along the geomagnetic field, to lower regions (i.e., E regions) of the ionosphere (both north and south of the equator). As these E regions build up conductivity they short out the polarization electric field associated with the long wavelength irregularities and so short out the irregularities. The time scale for the conductivity buildup would be shorter than the time required for these long wavelengths to disappear by diffusion.

ACKNOWLEDGMENTS

This work was supported by ONR and DNA.

REFERENCES

Aarons, J., J.P. Mullen, H.E. Whitney, and E.M. MacKenzie, The dynamics of equatorial irregularity patch formation, motion, and decay, J. Geophys. Res., 85, 139, 1980.

Basu, S., S. Basu, J. Aarons, J.P. McClure, and M.D. Cousins, On the coexistence of kilometer- and meter-scale irregularities in the nighttime equatorial F region, J. Geophys. Res., 83, 4219, 1978.

Basu, S., J.P. McClure, S. Basu, W.B. Hanson, and J. Aarons, Coordinated study of equatorial scintillation and in situ and radar observations of nighttime F region irregularities, J. Geophys. Res., 85, 5119, 1980.

Chaturvedi, P.K., and S.L. Ossakow, Nonlinear theory of the collisional Rayleigh-Taylor instability in equatorial spread F, Geophys. Res. Lett., 4, 558, 1977.

Costa, E., and M.C. Kelley, On the role of steepened structures and drift waves in equatorial spread F, J. Geophys. Res., 83, 4359, 1978a.

Costa, E., and M.C. Kelley, Linear theory for the collisionless drift wave instability with wavelengths near the ion gyroradius, J. Geophys. Res., 83, 4365, 1978b.

Farley, D.T., B.B. Balsley, R.F. Woodman, and J.P. McClure, Equatorial spread F: Implications of VHF radar observations, J. Geophys. Res., 75, 7199, 1970.

Gary, S.P., Waveparticle transport from electrostatic instabilities, Phys. Fluids, 23, 1193, 1980.

Goldman, S.R., and J.L. Sperling, Aspects of late-time striation behavior and satellite communication effects. Jaycor Report J78-2005-TR, 1979.

Haerendel, G., Theory of equatorial spread F, report, Max-Planck Inst. fur Phys. und Astrophys., Garching, West Germany, 1974.

Huba, J.D., and S.L. Ossakow, On the generation of 3 meter irregularities during equatorial spread F by low frequency drift waves. J. Geophys. Res., 84, 6697, 1979a.

Huba, J.D., and S.L. Ossakow, Destruction of cyclotron resonances in weakly collisional, inhomogeneous plasmas, Phys. Fluids, 22, 1349, 1979b.

Huba, J.D., and S.L. Ossakow, On 11 cm irregularities during equatorial spread F, J. Geophys. Res., 86, 829, 1981a.

Huba, J.D., and S.L. Ossakow, Physical mechanism of the lower-hybrid-drift instability in a collisional plasma, J. Atm. Terr. Phys., in press 1981b.

Huba, J.D., P.K. Chaturvedi, S.L. Ossakow, and D.M. Towle, High frequency drift waves with wavelengths below the ion gyroradius in equatorial spread F., Geophys. Res. Lett., 5 695, 1978.

Kadomtsev, B.B., Plasma Turbulence, Academic Press, New York, 1965.

Kelley, M.C., G. Haerendel, H. Kappler, A. Valenzuela, B.B. Balsley, D.A. Carter, W.L. Ecklund, C.W. Carlson, B. Hausler, and R. Torbert, Evidence for a Rayleigh-Taylor type

instability and upwelling of depleted density regions during equatorial spread F, Geophys. Res. Lett., 3, 448, 1976.

Kelley, M.C., R. Pfaff, K.D. Baker, J.C. Ulwick, R. Livingston, C. Rino, and R. Tsunoda, Simultaneous rocket probe and radar measurements of equatorial spread F-transitional and short wavelength results, J. Geophys. Res., submitted 1981.

Keskinen, M.J., S.L. Ossakow, and P.K. Chaturvedi, Preliminary report of numerical simulation of intermediate wavelength collisional Rayleigh-Taylor instability in equatorial spread F. J. Geophys. Res., 85, 1775, 1980.

Keskinen, M.J., E.P. Szuszczewicz, S.L. Ossakow, and J.C. Holmes, Nonlinear theory and experimental observations of the local collisional Rayleigh-Taylor instability in a descending equatorial spread-F ionosphere, J. Geophys. Res., in press 1981.

Longmire, C.L., Elementary Plasma Physics, Interscience Publishers, New York, 1963.

McClure, J.P., W.B. Hanson, and J.F. Hoffman, Plasma bubbles and irregularities in the equatorial ionosphere, J. Geophys. Res., 82, 2650, 1977.

Morse, F.A., B.C. Edgar, H.C. Koons, C.J. Rice, W.J. Heikkila, J.H. Hoffman, B.A. Tinsley, J.D. Winningham, A.B. Christensen, R.F. Woodman, J. Pomalaza, and N.R. Teixeira, Equion, an equatorial ionospheric irregularity experiment, J. Geophys. Res., 82, 578, 1977.

Ossakow, S.L., Spread F theories-a review, J. Atm. Terr. Phys.,

in press, 1981.

Ossakow, S.L., and P.K. Chaturvedi, Morphological studies of rising equatorial spread F bubbles, J. Geophys. Res., 83, 2085, 1978.

Ossakow. S.L., S.T. Zalesak, B.E. McDonald, and P.K. Chaturvedi, Nonlinear equatorial spread F: Dependence on altitude of the F peak and bottomside background electron density gradient scale length, J. Geophys. Res., 84, 17, 1979.

Ott, E., Theory of Rayleigh-Taylor bubbles in the equatorial ionosphere, J. Geophys. Res., 83, 2066, 1978.

Perkins, F.W., N.J. Zabusky, and J.H. Doles III, Deformation and striation of plasma clouds in the ionosphere, 1, J. Geophys. Res., 78, 697, 1973.

Rino, C.L., R.T. Tsunoda, J. Petriceks, R.C. Livingston, M.C. Kelley, and K.D. Baker, Simultaneous rocket-borne beacon and in-situ measurements of equatorial spread F--long wavelength results, J. Geophys. Res., in press, 1981.

Scannapieco. A.J., and S.L. Ossakow, Nonlinear equatorial spread F, Geophys. Res. Lett., 3, 451, 1976.

Sperling, J.L., and Goldman, S.R., Electron collisional effects on lower-hybrid-drift instabilities in the ionosphere, J. Geophys. Res., 85, 3494, 1980.

Szuszczewicz, E.P., R.T. Tsunoda, R. Narcisi, and J.C. Holmes, Coincident radar and rocket observations of equatorial spread F, Geophys. Res. Lett., 7, 537, 1980.

Towle, D.M., VHF and UHF radar obsrevations of equatorial ionospheric irregularities and background densities, Radio Sci.,

15, 71, 1980.

Tsunoda, R.T., Backscatter measurements of 11 cm equatorial spread F irregularities, Geophys. Res. Lett., 7, 848, 1980.

Tsunoda, R.T., Time evolution and dynamics of equatorial backscatter plumes, 1, Growth phase, J. Geophysical Res., 86, 139, 1981.

Tsunoda, R.T., and D.M. Towle, On the spatial relationship of 1-meter equatorial spread F irregularities and depletions in total electron content, Geophys. Res. Lett., 6, 873, 1979.

Weber, E.J., J. Buchau, R.H. Eather, and S.B. Mende, North-south aligned equatorial airglow depletions, J. Geophys. Res., 83, 712, 1978.

Woodman, R.F., and S. Basu, Comparision between in-situ spectral measurements of F region irregularities and backscatter observations at 3 m wavelength, Geophys. Res. Lett., 5, 869, 1978.

Zalesak, S.T., and S.L. Ossakow, Nonlinear equatorial spread F: Spatially large bubbles resulting from large horizontal scale initial perturbations, J. Geophys. Res., 85, 2131, 1980.

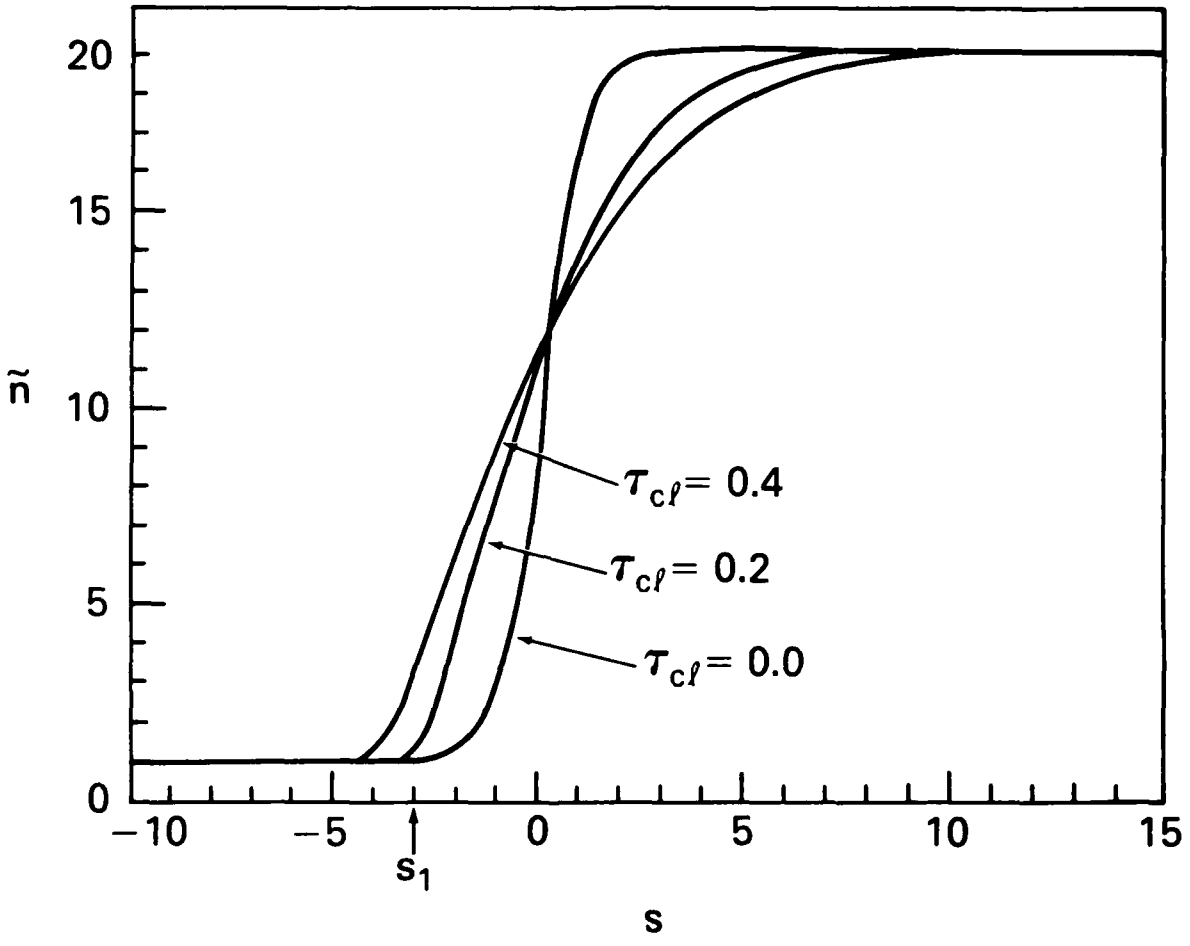

Fig. 1 — Classical diffusion process showing $\tilde{n}(s, \tau)$ vs. s for $\tau_{c\ell}$ = 0.0, 0.2, 0.4

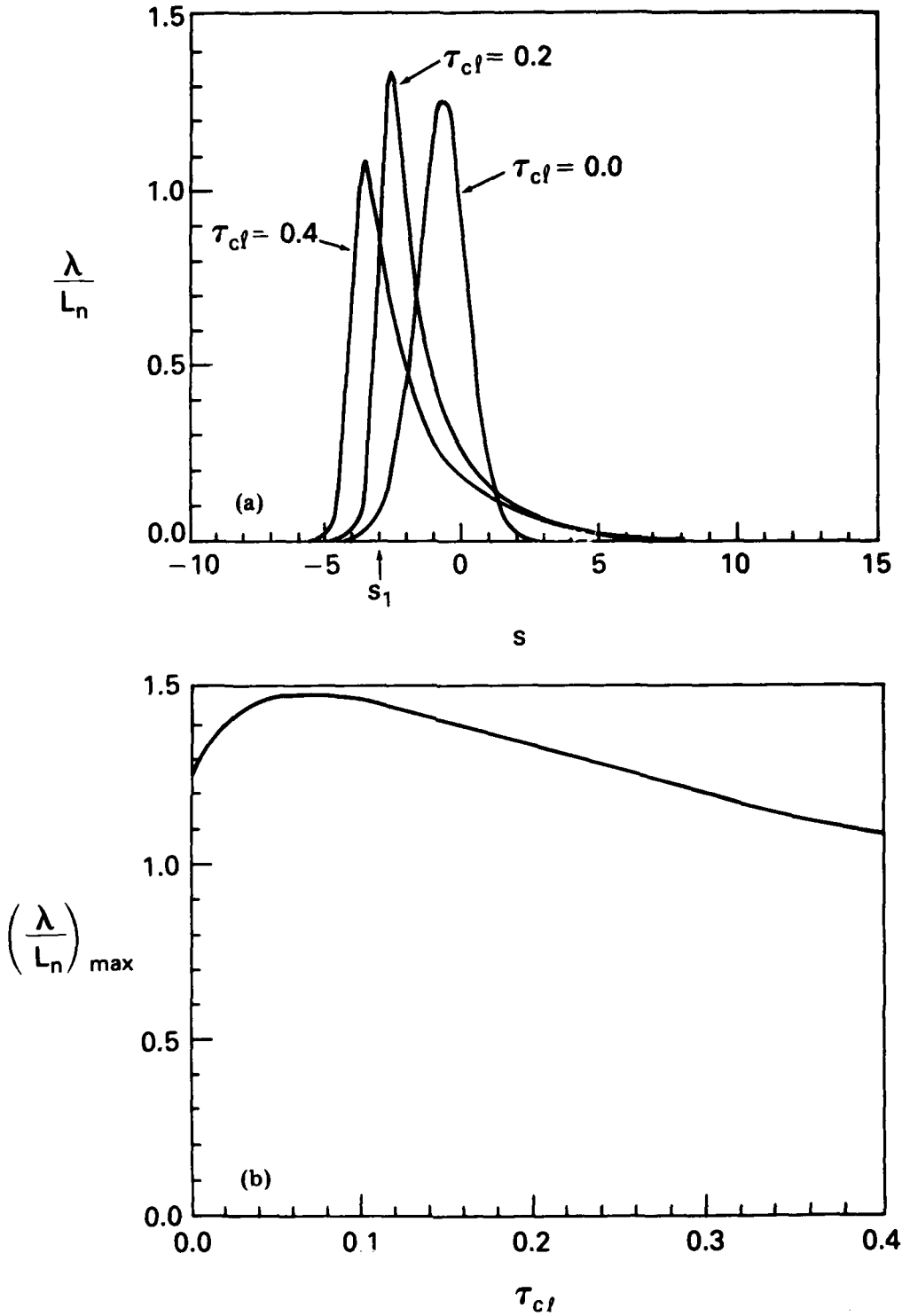

Fig. 2 — Spatial and temporal evolution of λ/L_n, the inverse scale length of the density gradient, for a classical diffusion process. (a) Spatial evolution of λ/L_n vs. s. (b) Temporal evolution of maximum inverse gradient scale length $(\lambda/L_n)_{max}$.

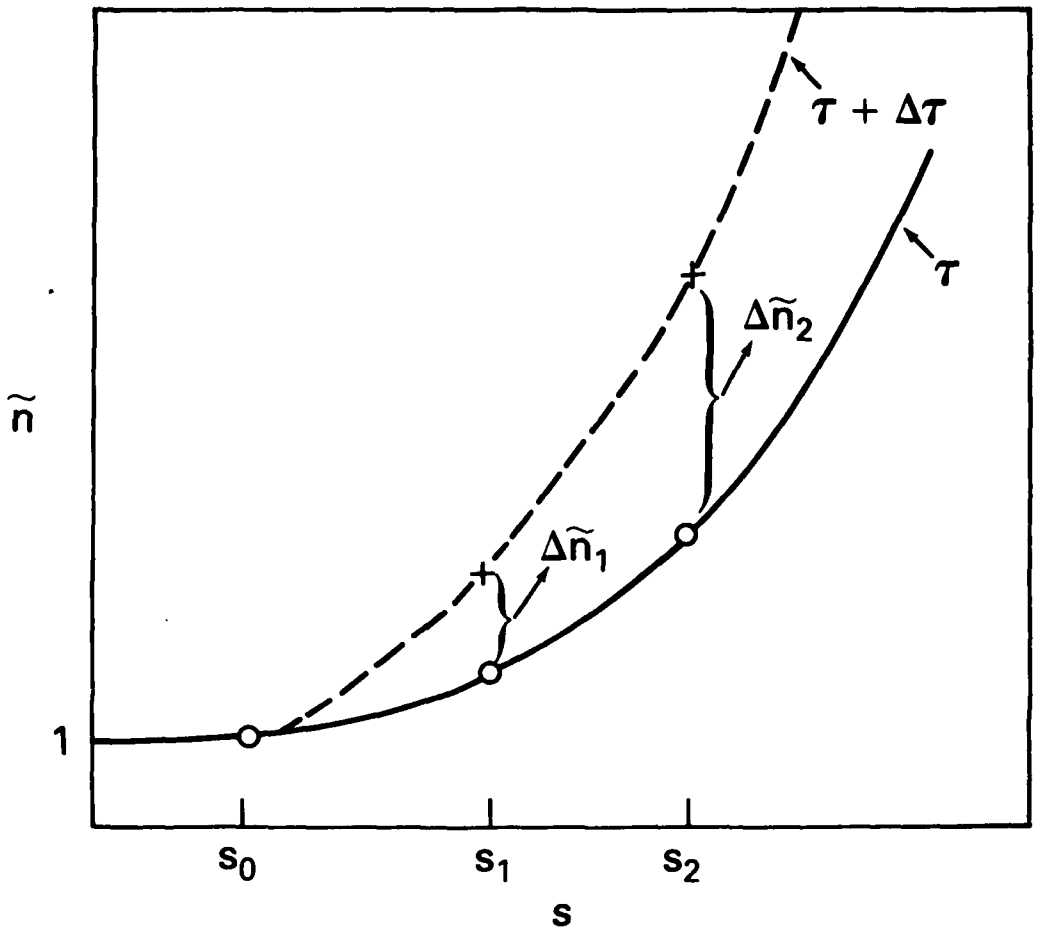

Fig. 3 — Schematic of $\tilde{n}$ vs. s to show initial steepening of the density profile

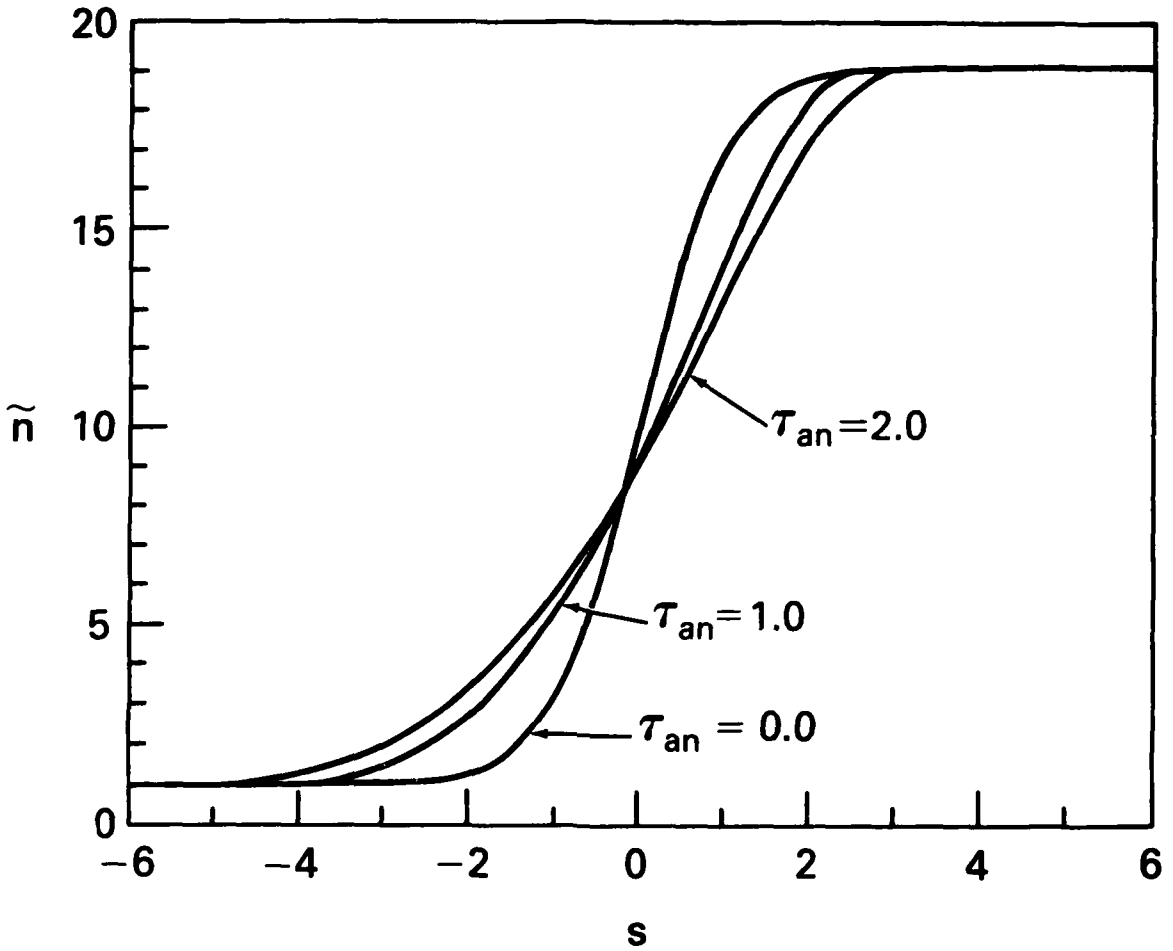

Fig. 4 — Anomalous diffusion process showing $\tilde{n}(s, \tau)$ vs. s for τ_{an} = 0.0, 1.0, 2.0

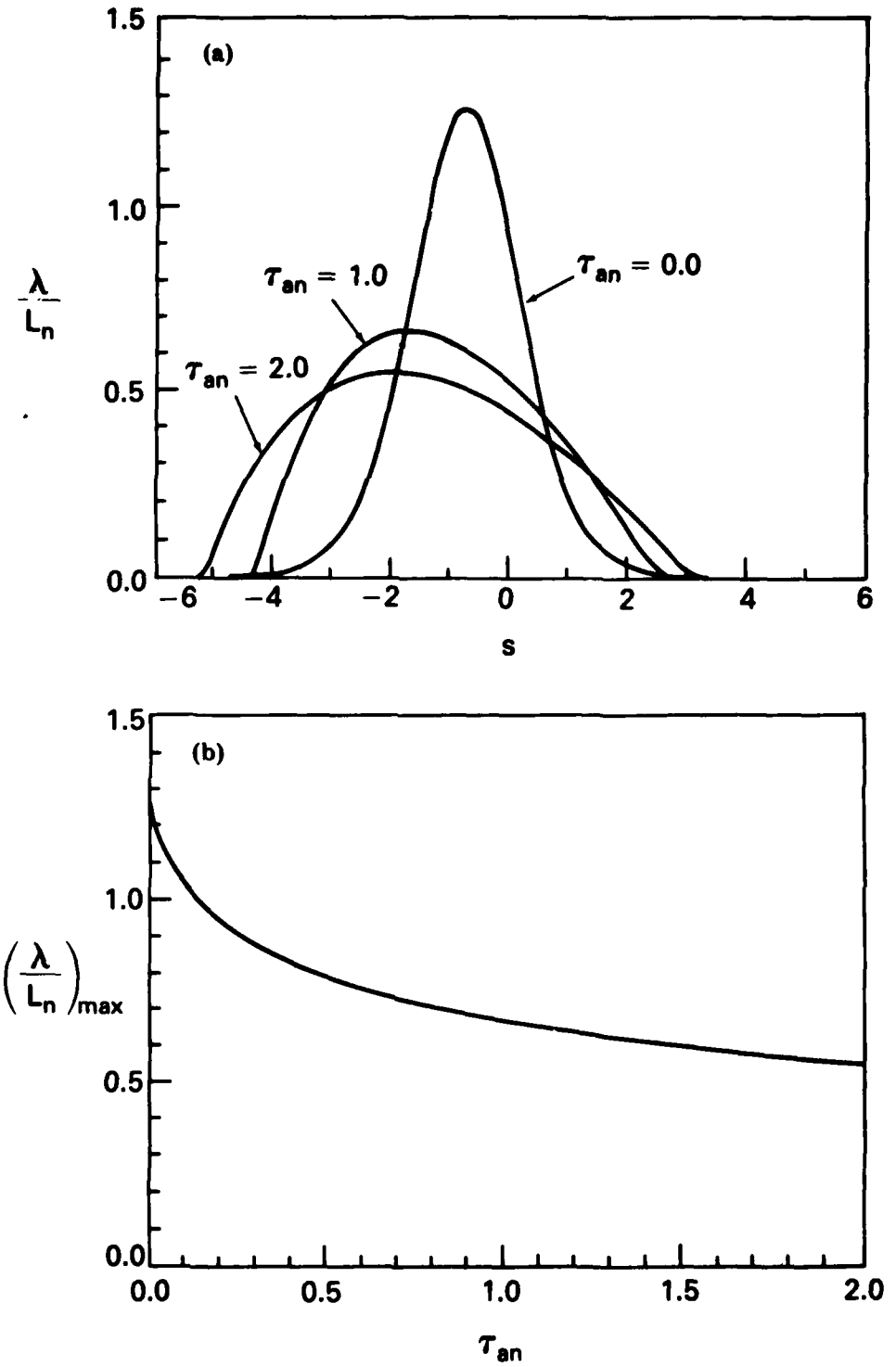

Fig. 5 — Spatial and temporal evolution of λ/L_n for an anomalous diffusion process. (a) Spatial evolution of λ/L_n vs. s. (b) Temporal evolution of $(\lambda/L_n)_{max}$.

TABLE 1. Classical and Anomalous Diffusion Time Scales for Parameters Typical of Equatorial Spread F

CLASSICAL DIFFUSION

	$\tau = 0.0$	$\tau = 0.2$		$\tau = 0.4$	
λ(m)	L_n(m)	L_n(m)	$t_{c\ell}$(hrs)	L_n(m)	$t_{c\ell}$(hrs)
50	40	38	0.9	47	1.8
100	80	76	3.5	94	7.0
200	160	152	14.0	188	28.0
500	400	380	90.0	470	180.0

ANOMALOUS DIFFUSION

	$\tau = 0.0$	$\tau = 1.0$		$\tau = 2.0$	
λ(m)	L_n(m)	L_n(m)	t_{an}(min)	L_n(m)	t_{an}(min)
50	40	71	0.1	90	0.2
100	80	142	0.9	181	1.8
200	160	285	6.9	363	13.9
500	400	714	108.0	909	216.0

APPENDIX

We present similarity solutions to the nonlinear classical and anomalous diffusion equations (Eqs. (10) and (11)).

1. Classical Diffusion

The classical diffusion equation, i.e., based on the Coulomb electron-ion collision frequency, has received considerable attention. A variety of similarity solutions exist depending upon the initial conditions and the boundary conditions. One solution is given in Longmire (1963).

We consider the equation (which is (14) recast)

$$\frac{\partial \tilde{n}}{\partial \tau} = \frac{1}{2} \frac{\partial^2 \tilde{n}^2}{\partial s^2} \tag{A1}$$

and search for solutions of the form

$$\tilde{n} = \tau^a \tilde{n} (s/\tau^b) \tag{A2}$$

where a and b are constants, Defining a new variable

$$\xi \equiv s/\tau^b \tag{A3}$$

and substituting Eqs. (A2) and (A3) into Eq. (A1) yields

$$a\tau^{a-1} \tilde{n}(\xi) - b\tau^{a-1} \xi \frac{\partial \tilde{n}}{\partial \xi} = \frac{1}{2}\tau^{2a-2b} \frac{\partial^2 \tilde{n}}{\partial \xi^2} \tag{A4}$$

We require

$$a = 2b - 1 \tag{A5}$$

so that the powers of t cancel. In order to determine a and b we impose the added condition that the plasma can diffuse freely (i.e., $\int \tilde{n} ds$ = constant), This leads to the requirement that

$$a + b = 0 \tag{A6}$$

Thus, from Eqs. (A5) and (A6) we obtain

$$a = -1/3; \quad b = 1/3 \tag{A7}$$

and Eq. (A4) becomes

$$-\frac{1}{3}\,\tilde{n}(\xi) - \frac{1}{3}\,\xi\,\frac{\partial \tilde{n}}{\partial \xi} = \frac{1}{2}\,\frac{\partial^2 \tilde{n}^2}{\partial \xi^2}\,. \tag{A8}$$

The solutions of Eq. (A8) require $\tilde{n}$ vanish at some point so that the plasma occupies a finite region at any time. We choose $s = \pm s_o$ (the vanishing point) at $\tau = \tau_o$. The density is then given by

$$\tilde{n}\,(s,\tau) = \frac{s_o^{\,2}}{6\tau_o^{\,2/3}\tau^{1/3}}\left[1 - \left(\frac{s}{s_o}\right)^2\left(\frac{\tau_o}{\tau}\right)^{2/3}\right] \tag{A9}$$

Note that if the initial density at the origin is $\tilde{n}_o = 1$ and the initial scale length is $s_o = 1$ ($x \sim \lambda$), the time it takes for the scale length to double is

$$\Delta\tau_{c\ell} \sim \frac{7}{6} \tag{A10}$$

or

$$\Delta t_{c\ell} \sim \frac{7}{6}\,\frac{\lambda^2}{\rho_{es}^{\,2}}\,\frac{1}{\nu_{c\ell}^{o}} \tag{A11}$$

which is comparable to the numerical results. It is important to recognize a major difference between the similarity solution Eq. (A9) and the ionospheric problem. Equation (A9) considers the diffusion of a density enhancement as opposed to a density depletion which occurs in the ionosphere. One difference is the initial steepening of the density profile for a depletion. This effect does not occur for an enhancement. However, the asymptotic solutions of both problems yield comparable time scales.

2. Anomalous Diffusion

We consider the equation

$$\frac{\partial \tilde{n}}{\partial \tau} = \frac{\partial}{\partial s}\left(\left| \frac{1}{\tilde{n}} \quad \frac{\partial \tilde{n}}{\partial s} \right| \quad \frac{\partial \tilde{n}}{\partial s} \right) \tag{A12}$$

and look for solutions of the form

$$\tilde{n} = 1 - \delta \exp\left(-\psi(\chi)\right) \tag{A13}$$

where $\chi = s^a/\tau^b$ and $0<\delta<1$ substituting Eq (A13) into Eq. (A12), we find $a = 3$ and $b = 1$ where $\psi(\chi)$ satisfies the nonlinear differential equation

$$\chi\left(\frac{d\psi}{d\chi}\right)^2 - \frac{4}{3}\frac{d\psi}{d\chi} - 2\chi\frac{d^2\psi}{d\chi^2} = 1 \tag{A14}$$

For large χ, the solution to Eq. (A14) is

$$\psi = \chi^{\frac{1}{2}} + 0\left(\frac{1}{\chi^{\frac{1}{2}}}\right) \tag{A15}$$

or

$$\tilde{n} = 1 - \delta \exp \left[- (s^3/\tau)^{\frac{1}{2}} \right] \qquad \text{(A16)}$$

This solution more closely resembles the ionospheric problem since it represents a density depletion being filled with plasma. Equation (A16) predicts that the scale length of the density sheath broadens at a rate proportional to $\tau_{an}^{1/3}$. This is slightly faster then the results shown in Figure 5 for $(\lambda/L_n)_{max}$ vs. τ_{an} which is not surprising owing to the approximations made in obtaining Eq. (A16).

DISTRIBUTION LIST

DEPARTMENT OF DEFENSE

ASSISTANT SECRETARY OF DEFENSE
COMM, CMD, CONT & INTELL
WASHINGTON, D.C. 20301
01CY ATTN J. BABCOCK
01CY ATTN M. EPSTEIN

DIRECTOR
COMMAND CONTROL TECHNICAL CENTER
PENTAGON RM BE 685
WASHINGTON, D.C. 20301
01CY ATTN C-650
01CY ATTN C-312 R. MASON

DIRECTOR
DEFENSE ADVANCED RSCH PROJ AGENCY
ARCHITECT BUILDING
1400 WILSON BLVD.
ARLINGTON, VA. 22209
01CY ATTN NUCLEAR MONITORING RESEARCH
01CY ATTN STRATEGIC TECH OFFICE

DEFENSE COMMUNICATION ENGINEER CENTER
1860 WIEHLE AVENUE
RESTON, VA. 22090
01CY ATTN CODE R820
01CY ATTN CODE R410 JAMES W. MCLEAN
01CY ATTN CODE R720 J. WORTHINGTON

DIRECTOR
DEFENSE COMMUNICATIONS AGENCY
WASHINGTON, D.C. 20305
(ADR CNWDI: ATTN CODE 240 FOR)
01CY ATTN CODE 101B

DEFENSE TECHNICAL INFORMATION CENTER
CAMERON STATION
ALEXANDRIA, VA. 22314
(12 COPIES IF OPEN PUBLICATION, OTHERWISE 2 COPIES)
12CY ATTN TC

DIRECTOR
DEFENSE INTELLIGENCE AGENCY
WASHINGTON, D.C. 20301
01CY ATTN DT-1B
01CY ATTN DB-4C E. O'FARRELL
01CY ATTN DIAAP A. WISE
01CY ATTN DIAST-5
01CY ATTN DT-1BZ K. MORTON
01CY ATTN HQ-TR J. STEWART
01CY ATTN W. WITTIG DC-7D

DIRECTOR
DEFENSE NUCLEAR AGENCY
WASHINGTON, D.C. 20305
01CY ATTN STVL
04CY ATTN TITL
01CY ATTN DDST
03CY ATTN RAAE

COMMANDER
FIELD COMMAND
DEFENSE NUCLEAR AGENCY
KIRTLAND AFB, NM 87115
01CY ATTN FCPR

DIRECTOR
INTERSERVICE NUCLEAR WEAPONS SCHOOL
KIRTLAND AFB, NM 87115
01CY ATTN DOCUMENT CONTROL

OJCS, C3S EVALUATION OFFICE
Washington, D.C. 20301

DIRECTOR
JOINT STRAT TGT PLANNING STAFF
OFFUTT AFB
OMAHA, NB 68113
01CY ATTN JLTW-2
01CY ATTN JPST G. GOETZ

CHIEF
LIVERMORE DIVISION FLD COMMAND DNA
DEPARTMENT OF DEFENSE
LAWRENCE LIVERMORE LABORATORY
P. O. BOX 808
LIVERMORE, CA 94550
01CY ATTN FCPRL

DIRECTOR
NATIONAL SECURITY AGENCY
DEPARTMENT OF DEFENSE
FT. GEORGE G. MEADE, MD 20755
01CY ATTN JOHN SKILLMAN R52
01CY ATTN FRANK LEONARD
01CY ATTN W14 PAT CLARK
01CY ATTN OLIVER H. BARTLETT W32
01CY ATTN R5

COMMANDANT
NATO SCHOOL (SHAPE)
APO NEW YORK 09172
01CY ATTN U.S. DOCUMENTS OFFICER

UNDER SECY OF DEF FOR RSCH & ENGRG
DEPARTMENT OF DEFENSE
WASHINGTON, D.C. 20301
01CY ATTN STRATEGIC & SPACE SYSTEMS (OS)

WWMCCS SYSTEM ENGINEERING ORG
WASHINGTON, D.C. 20305
01CY ATTN R. CRAWFORD

COMMANDER/DIRECTOR
ATMOSPHERIC SCIENCES LABORATORY
U.S. ARMY ELECTRONICS COMMAND
WHITE SANDS MISSILE RANGE, NM 88002
01CY ATTN DELAS-EO F. NILES

DIRECTOR
BMD ADVANCED TECH CTR
HUNTSVILLE OFFICE
P. O. BOX 1500
HUNTSVILLE, AL 35807
01CY ATTN ATC-T MELVIN T. CAPPS
01CY ATTN ATC-O W. DAVIES
01CY ATTN ATC-R DON RUSS

PROGRAM MANAGER
BMD PROGRAM OFFICE
5001 EISENHOWER AVENUE
ALEXANDRIA, VA 22333
01CY ATTN DACS-BMT J. SHEA

CHIEF C-E SERVICES DIVISION
U.S. ARMY COMMUNICATIONS CMD
PENTAGON RM 1B269
WASHINGTON, D.C. 20310
01CY ATTN C-E-SERVICES DIVISION

COMMANDER
FRADCOM TECHNICAL SUPPORT ACTIVITY
DEPARTMENT OF THE ARMY
FORT MONMOUTH, N.J. 07703
01CY ATTN DRSEL-NL-RD H. BENNET
01CY ATTN DRSEL-PL-ENV M. BOMKE
01CY ATTN J. E. QUIGLEY

COMMANDER
HARRY DIAMOND LABORATORIES
DEPARTMENT OF THE ARMY
2800 POWDER MILL ROAD
ADELPHI, MD 20783
(CNWDI-INNER ENVELOPE: ATTN: DELHD-KBH)
01CY ATTN DELHD-TI M. WEINER
01CY ATTN DELHD-RB R. WILLIAMS
01CY ATTN DELHD-NP F. WIMENITZ
01CY ATTN DELHD-NP C. MOAZED

COMMANDER
U.S. ARMY COMM-ELEC ENGRG INSTAL AGY
FT. HUACHUCA, AZ 85613
01CY ATTN CCC-EMEO GEORGE LANE

COMMANDER
U.S. ARMY FOREIGN SCIENCE & TECH CTR
220 7TH STREET, NE
CHARLOTTESVILLE, VA 22901
01CY ATTN DRXST-SD
01CY ATTN R. JONES

COMMANDER
U.S. ARMY MATERIEL DEV & READINESS CMD
5001 EISENHOWER AVENUE
ALEXANDRIA, VA 22333
01CY ATTN DRCLDC J. A. BENDER

COMMANDER
U.S. ARMY NUCLEAR AND CHEMICAL AGENCY
7500 BACKLICK ROAD
BLDG 2073
SPRINGFIELD, VA 22150
01CY ATTN LIBRARY

DIRECTOR
U.S. ARMY BALLISTIC RESEARCH LABS
ABERDEEN PROVING GROUND, MD 21005
01CY ATTN TECH LIB EDWARD BAICY

COMMANDER
U.S. ARMY SATCOM AGENCY
FT. MONMOUTH, NJ 07703
01CY ATTN DOCUMENT CONTROL

COMMANDER
U.S. ARMY MISSILE INTELLIGENCE AGENCY
REDSTONE ARSENAL, AL 35809
01CY ATTN JIM GAMBLE

DIRECTOR
U.S. ARMY TRADOC SYSTEMS ANALYSIS ACTIVITY
WHITE SANDS MISSILE RANGE, NM 88002
01CY ATTN ATAA-SA
01CY ATTN TCC/F. PAYAN JR.
01CY ATTN ATAA-TAC LTC J. HESSE

COMMANDER
NAVAL ELECTRONIC SYSTEMS COMMAND
WASHINGTON, D.C. 20360
01CY ATTN NAVALEX 034 T. HUGHES
01CY ATTN PME 117
01CY ATTN PME 117-T
01CY ATTN CODE 5011

COMMANDING OFFICER
NAVAL INTELLIGENCE SUPPORT CTR
4301 SUITLAND ROAD, BLDG. 5
WASHINGTON, D.C. 20390
01CY ATTN MR. DUBBIN STIC 12
01CY ATTN NISC-50
01CY ATTN CODE 5404 J. JALET

COMMANDER
NAVAL OCEAN SYSTEMS CENTER
SAN DIEGO, CA 92152
03CY ATTN CODE 532 W. MOLER
01CY ATTN CODE 0230 C. BAGGETT
01CY ATTN CODE 81 K. EASTMAN

DIRECTOR
NAVAL RESEARCH LABORATORY
WASHINGTON, D.C. 20375
01CY ATTN CODE 4700 T. P. COFFEY (25 CYS)
01CY ATTN CODE 4701 JACK D. BROWN
01CY ATTN CODE 4780 BRANCH HEAD (150 CYS)
01CY ATTN CODE 7500
01CY ATTN CODE 7550
01CY ATTN CODE 7580
01CY ATTN CODE 7551
01CY ATTN CODE 7555
01CY ATTN CODE 4730 E. MCLEAN
01CY ATTN CODE 4187

COMMANDER
NAVAL SEA SYSTEMS COMMAND
WASHINGTON, D.C. 20362
01CY ATTN CAPT R. PITKIN

COMMANDER
NAVAL SPACE SURVEILLANCE SYSTEM
DAHLGREN, VA 22448
01CY ATTN CAPT J. H. BURTON

OFFICER-IN-CHARGE
NAVAL SURFACE WEAPONS CENTER
WHITE OAK, SILVER SPRING, MD 20910
01CY ATTN CODE F31

DIRECTOR
STRATEGIC SYSTEMS PROJECT OFFICE
DEPARTMENT OF THE NAVY
WASHINGTON, D.C. 20376
01CY ATTN NSP-2141
01CY ATTN NSSP-2722 FRED WIMBERLY

COMMANDER
NAVAL SURFACE WEAPONS CENTER
DAHLGREN LABORATORY
DAHLGREN, VA 22448
01CY ATTN CODE DF-14 R. BUTLER

OFFICE OF NAVAL RESEARCH
ARLINGTON, VA 22217
01CY ATTN CODE 465
01CY ATTN CODE 461
01CY ATTN CODE 402
01CY ATTN CODE 420
01CY ATTN CODE 421

COMMANDER
AEROSPACE DEFENSE COMMAND/DC
DEPARTMENT OF THE AIR FORCE
ENT AFB, CO 80912
01CY ATTN DC MR. LONG

COMMANDER
AEROSPACE DEFENSE COMMAND/XPD
DEPARTMENT OF THE AIR FORCE
ENT AFB, CO 80912
01CY ATTN XPDQQ
01CY ATTN XP

AIR FORCE GEOPHYSICS LABORATORY
HANSCOM AFB, MA 01731
01CY ATTN OPR HAROLD GARDNER
01CY ATTN OPR-1 JAMES C. ULWICK
01CY ATTN LKB KENNETH S. W. CHAMPION
01CY ATTN OPR ALVA T. STAIR
01CY ATTN PHP JULES AARONS
01CY ATTN PHD JURGEN BUCHAU
01CY ATTN PHD JOHN P. MULLEN

AF WEAPONS LABORATORY
KIRTLAND AFB, NM 87117
01CY ATTN SUL
01CY ATTN CA ARTHUR H. GUENTHER
01CY ATTN NTYC 1LT G. KRAJCI

AFTAC
PATRICK AFB, FL 32925
01CY ATTN TF/MAJ WILEY
01CY ATTN TN

AIR FORCE AVIONICS LABORATORY
WRIGHT-PATTERSON AFB, OH 45433
01CY ATTN AAD WADE HUNT
01CY ATTN AAD ALLEN JOHNSON

DEPUTY CHIEF OF STAFF
RESEARCH, DEVELOPMENT, & ACQ
DEPARTMENT OF THE AIR FORCE
WASHINGTON, D.C. 20330
01CY ATTN AFRDQ

HEADQUARTERS
ELECTRONIC SYSTEMS DIVISION/XR
DEPARTMENT OF THE AIR FORCE
HANSCOM AFB, MA 01731
01CY ATTN XR J. DEAS

HEADQUARTERS
ELECTRONIC SYSTEMS DIVISION/YSEA
DEPARTMENT OF THE AIR FORCE
HANSCOM AFB, MA 01732
01CY ATTN YSEA

HEADQUARTERS
ELECTRONIC SYSTEMS DIVISION/DC
DEPARTMENT OF THE AIR FORCE
HANSCOM AFB, MA 01731
01CY ATTN DCKC MAJ J.C. CLARK

COMMANDER
FOREIGN TECHNOLOGY DIVISION, AFSC
WRIGHT-PATTERSON AFB, OH 45433
01CY ATTN NICD LIBRARY
01CY ATTN ETDP B. BALLARD

COMMANDER
ROME AIR DEVELOPMENT CENTER, AFSC
GRIFFISS AFB, NY 13441
01CY ATTN DOC LIBRARY/TSLD
01CY ATTN OCSE V. COYNE

SAMSO/SZ
POST OFFICE BOX 92960
WORLDWAY POSTAL CENTER
LOS ANGELES, CA 90009
(SPACE DEFENSE SYSTEMS)
01CY ATTN SZJ

STRATEGIC AIR COMMAND/XPFS
OFFUTT AFB, NB 68113
01CY ATTN XPFS MAJ B. STEPHAN
01CY ATTN ADWATE MAJ BRUCE BAUER
01CY ATTN NRT
01CY ATTN DOK CHIEF SCIENTIST

SAMSO/SK
P. O. BOX 92960
WORLDWAY POSTAL CENTER
LOS ANGELES, CA 90009
01CY ATTN SKA (SPACE COMM SYSTEMS) M. CLAVIN

SAMSO/MN
NORTON AFB, CA 92409
(MINUTEMAN)
01CY ATTN MNNL LTC KENNEDY

COMMANDER
ROME AIR DEVELOPMENT CENTER, AFSC
HANSCOM AFB, MA 01731
01CY ATTN EEP A. LORENTZEN

DEPARTMENT OF ENERGY
ALBUQUERQUE OPERATIONS OFFICE
P. O. BOX 5400
ALBUQUERQUE, NM 87115
01CY ATTN DOC CON FOR D. SHERWOOD

DEPARTMENT OF ENERGY
LIBRARY ROOM G-042
WASHINGTON, D.C. 20545
01CY ATTN DOC CON FOR A. LABOWITZ

EG&G, INC.
LOS ALAMOS DIVISION
P. O. BOX 809
LOS ALAMOS, NM 85544
01CY ATTN DOC CON FOR J. BREEDLOVE

UNIVERSITY OF CALIFORNIA
LAWRENCE LIVERMORE LABORATORY
P. O. BOX 808
LIVERMORE, CA 94550
01CY ATTN DOC CON FOR TECH INFO DEPT
01CY ATTN DOC CON FOR L-389 R. OTT
01CY ATTN DOC CON FOR L-31 R. HAGER
01CY ATTN DOC CON FOR L-46 F. SEWARD

LOS ALAMOS SCIENTIFIC LABORATORY
P. O. BOX 1663
LOS ALAMOS, NM 87545
01CY ATTN DOC CON FOR J. WOLCOTT
01CY ATTN DOC CON FOR R. F. TASCHEK
01CY ATTN DOC CON FOR E. JONES
01CY ATTN DOC CON FOR J. MALIK
01CY ATTN DOC CON FOR R. JEFFRIES
01CY ATTN DOC CON FOR J. ZINN
01CY ATTN DOC CON FOR P. KEATON
01CY ATTN DOC CON FOR D. WESTERVELT

SANDIA LABORATORIES
P. O. BOX 5800
ALBUQUERQUE, NM 87115
01CY ATTN DOC CON FOR J. MARTIN
01CY ATTN DOC CON FOR W. BROWN
01CY ATTN DOC CON FOR A. THORNBROUGH
01CY ATTN DOC CON FOR T. WRIGHT
01CY ATTN DOC CON FOR D. DAHLGREN
01CY ATTN DOC CON FOR 3141
01CY ATTN DOC CON FOR SPACE PROJECT DIV

SANDIA LABORATORIES
LIVERMORE LABORATORY
P. O. BOX 969
LIVERMORE, CA 94550
01CY ATTN DOC CON FOR B. MURPHEY
01CY ATTN DOC CON FOR T. COOK

OFFICE OF MILITARY APPLICATION
DEPARTMENT OF ENERGY
WASHINGTON, D.C. 20545
01CY ATTN DOC CON FOR D. GALE

OTHER GOVERNMENT

CENTRAL INTELLIGENCE AGENCY
ATTN RD/SI, RM 5G48, HQ BLDG
WASHINGTON, D.C. 20505
01CY ATTN OSI/PSID RM 5F 19

DEPARTMENT OF COMMERCE
NATIONAL BUREAU OF STANDARDS
WASHINGTON, D.C. 20234
(ALL CORRES: ATTN SEC OFFICER FOR)
01CY ATTN R. MOORE

INSTITUTE FOR TELECOM SCIENCES
NATIONAL TELECOMMUNICATIONS & INFO ADMIN
BOULDER, CO 80303
01CY ATTN A. JEAN (UNCLASS ONLY)
01CY ATTN W. UTLAUT
01CY ATTN D. CROMBIE
01CY ATTN L. BERRY

NATIONAL OCEANIC & ATMOSPHERIC ADMIN
ENVIRONMENTAL RESEARCH LABORATORIES
DEPARTMENT OF COMMERCE
BOULDER, CO 80302
01CY ATTN R. GRUBB
01CY ATTN AERONOMY LAB G. REID

DEPARTMENT OF DEFENSE CONTRACTORS

AEROSPACE CORPORATION
P. O. BOX 92957
LOS ANGELES, CA 90009
01CY ATTN I. GARFUNKEL
01CY ATTN T. SALMI
01CY ATTN V. JOSEPHSON
01CY ATTN S. BOWER
01CY ATTN N. STOCKWELL
01CY ATTN D. OLSEN
01CY ATTN SMFA FOR PWW

ANALYTICAL SYSTEMS ENGINEERING CORP
5 OLD CONCORD ROAD
BURLINGTON, MA 01803
01CY ATTN RADIO SCIENCES

BERKELEY RESEARCH ASSOCIATES, INC.
P. O. BOX 983
BERKELEY, CA 94701
01CY ATTN J. WORKMAN

BOEING COMPANY, THE
P. O. BOX 3707
SEATTLE, WA 98124
01CY ATTN G. KEISTER
01CY ATTN D. MURRAY
01CY ATTN G. HALL
01CY ATTN J. KENNEY

CALIFORNIA AT SAN DIEGO, UNIV OF
P.O. BOX 6049
SAN DIEGO, CA 92106

BROWN ENGINEERING COMPANY, INC.
CUMMINGS RESEARCH PARK
HUNTSVILLE, AL 35807
01CY ATTN ROMEO A. DELIBERIS

CHARLES STARK DRAPER LABORATORY, INC.
555 TECHNOLOGY SQUARE
CAMBRIDGE, MA 02139
01CY ATTN D. B. COX
01CY ATTN J. P. GILMORE

COMSAT LABORATORIES
LINTHICUM ROAD
CLARKSBURG, MD 20734
01CY ATTN G. HYDE

CORNELL UNIVERSITY
DEPARTMENT OF ELECTRICAL ENGINEERING
ITHACA, NY 14850
01CY ATTN D. T. FARLEY JR

ELECTROSPACE SYSTEMS, INC.
BOX 1359
RICHARDSON, TX 75080
01CY ATTN H. LOGSTON
01CY ATTN SECURITY (PAUL PHILLIPS)

ESL INC.
495 JAVA DRIVE
SUNNYVALE, CA 94086
01CY ATTN J. ROBERTS
01CY ATTN JAMES MARSHALL
01CY ATTN C. W. PRETTIE

GENERAL ELECTRIC COMPANY
SPACE DIVISION
VALLEY FORGE SPACE CENTER
GODDARD BLVD KING OF PRUSSIA
P. O. BOX 8555
PHILADELPHIA, PA 19101
01CY ATTN M. H. BORTNER SPACE SCI LAB

GENERAL ELECTRIC COMPANY
P. O. BOX 1122
SYRACUSE, NY 13201
01CY ATTN F. REIBERT

GENERAL ELECTRIC COMPANY
TEMPO-CENTER FOR ADVANCED STUDIES
816 STATE STREET (P.O. DRAWER QQ)
SANTA BARBARA, CA 93102
01CY ATTN DASIAC
01CY ATTN DON CHANDLER
01CY ATTN TOM BARRETT
01CY ATTN TIM STEPHANS
01CY ATTN WARREN S. KNAPP
01CY ATTN WILLIAM MCNAMARA
01CY ATTN B. GAMBILL
01CY ATTN MACK STANTON

GENERAL ELECTRIC TECH SERVICES CO., INC.
HMES
COURT STREET
SYRACUSE, NY 13201
01CY ATTN G. MILLMAN

GENERAL RESEARCH CORPORATION
SANTA BARBARA DIVISION
P. O. BOX 6770
SANTA BARBARA, CA 93111
01CY ATTN JOHN ISE JR
01CY ATTN JOEL GARBARINO

GEOPHYSICAL INSTITUTE
UNIVERSITY OF ALASKA
FAIRBANKS, AK 99701
(ALL CLASS ATTN: SECURITY OFFICER)
01CY ATTN T. N. DAVIS (UNCL ONLY)
01CY ATTN NEAL BROWN (UNCL ONLY)
01CY ATTN TECHNICAL LIBRARY

GTE SYLVANIA, INC.
ELECTRONICS SYSTEMS GRP-EASTERN DIV
77 A STREET
NEEDHAM, MA 02194
01CY ATTN MARSHAL CROSS

ILLINOIS, UNIVERSITY OF
107 COBLE HALL
150 DAVENPORT HOUSE
CHAMPAIGN, IL 61820
(ALL CORRES ATTN DAN MCCLELLAND)
01CY FOR K. YEH

INSTITUTE FOR DEFENSE ANALYSES
400 ARMY-NAVY DRIVE
ARLINGTON, VA 22202
01CY ATTN J. M. AEIN
01CY ATTN ERNEST BAUER
01CY ATTN HANS WOLFHARD
01CY ATTN JOEL BENGSTON

HSS, INC.
2 ALFRED CIRCLE
BEDFORD, MA 01730
01CY ATTN DONALD HANSEN

INTL TEL & TELEGRAPH CORPORATION
500 WASHINGTON AVENUE
NUTLEY, NJ 07110
01CY ATTN TECHNICAL LIBRARY

JAYCOR
1401 CAMINO DEL MAR
DEL MAR, CA 92014
01CY ATTN S. R. GOLDMAN

JOHNS HOPKINS UNIVERSITY
APPLIED PHYSICS LABORATORY
JOHNS HOPKINS ROAD
LAUREL, MD 20810
01CY ATTN DOCUMENT LIBRARIAN
01CY ATTN THOMAS POTEMRA
01CY ATTN JOHN DASSOULAS

LOCKHEED MISSILES & SPACE CO INC
P. O. BOX 504
SUNNYVALE, CA 94088
01CY ATTN DEPT 60-12
01CY ATTN D. R. CHURCHILL

LOCKHEED MISSILES AND SPACE CO INC
3251 HANOVER STREET
PALO ALTO, CA 94304
01CY ATTN MARTIN WALT DEPT 52-10
01CY ATTN RICHARD G. JOHNSON DEPT 52-12
01CY ATTN W. L. IMHOF DEPT 52-12

KAMAN SCIENCES CORP
P. O. BOX 7463
COLORADO SPRINGS, CO 80933
01CY ATTN T. MEAGHER

LINKABIT CORP
10453 ROSELLE
SAN DIEGO, CA 92121
01CY ATTN IRWIN JACOBS

M.I.T. LINCOLN LABORATORY
P. O. BOX 73
LEXINGTON, MA 02173
01CY ATTN DAVID M. TOWLE
01CY ATTN P. WALDRON
01CY ATTN L. LOUGHLIN
01CY ATTN D. CLARK

MARTIN MARIETTA CORP
ORLANDO DIVISION
P. O. BOX 5837
ORLANDO, FL 32805
01CY ATTN R. HEFFNER

PHYSICAL DYNAMICS INC.
P. O. BOX 3027
BELLEVUE, WA 98009
01CY ATTN E. J. FREMOUW

PHYSICAL DYNAMICS INC.
P. O. BOX 10367
OAKLAND, CA. 94610
ATTN: A. THOMSON

R & D ASSOCIATES
P. O. BOX 9695
MARINA DEL REY, CA 90291
01CY ATTN FORREST GILMORE
01CY ATTN BRYAN GABBARD
01CY ATTN WILLIAM B. WRIGHT JR
01CY ATTN ROBERT F. LELEVIER
01CY ATTN WILLIAM J. KARZAS
01CY ATTN H. ORY
01CY ATTN C. MACDONALD
01CY ATTN R. TURCO

RAND CORPORATION, THE
1700 MAIN STREET
SANTA MONICA, CA 90406
01CY ATTN CULLEN CRAIN
01CY ATTN ED BEDROZIAN

RIVERSIDE RESEARCH INSTITUTE
80 WEST END AVENUE
NEW YORK, NY 10023
01CY ATTN VINCE TRAPANI

SCIENCE APPLICATIONS, INC.
P. O. BOX 2351
LA JOLLA, CA 92038
01CY ATTN LEWIS M. LINSON
01CY ATTN DANIEL A. HAMLIN
01CY ATTN D. SACHS
01CY ATTN E. A. STRAKER
01CY ATTN CURTIS A. SMITH
01CY ATTN JACK MCDOUGALL

RAYTHEON CO.
528 BOSTON POST ROAD
SUDBURY, MA 01776
01CY ATTN BARBARA ADAMS

SCIENCE APPLICATIONS, INC.
1710 GOODRIDGE DR.
MCLEAN, VA 22102
ATTN: J. COCKAYNE

LOCKHEED MISSILE & SPACE CO., INC.
HUNTSVILLE RESEARCH & ENGR. CTR.
4800 BRADFORD DRIVE
HUNTSVILLE, ALABAMA 35807
ATTN: DALE H. DAVIS

MCDONNELL DOUGLAS CORPORATION
5301 BOLSA AVENUE
HUNTINGTON BEACH, CA 92647
01CY ATTN N. HARRIS
01CY ATTN J. MOULE
01CY ATTN GEORGE MROZ
01CY ATTN W. OLSON
01CY ATTN R. W. HALPRIN
01CY ATTN TECHNICAL LIBRARY SERVICES

MISSION RESEARCH CORPORATION
735 STATE STREET
SANTA BARBARA, CA 93101
01CY ATTN P. FISCHER
01CY ATTN W. F. CREVIER
01CY ATTN STEVEN L. GUTSCHE
01CY ATTN D. SAPPENFIELD
01CY ATTN R. BOGUSCH
01CY ATTN R. HENDRICK
01CY ATTN RALPH KILB
01CY ATTN DAVE SOWLE
01CY ATTN F. FAJEN
01CY ATTN M. SCHEIBE
01CY ATTN CONRAD L. LONGMIRE
01CY ATTN WARREN A. SCHLUETER

MITRE CORPORATION, THE
P. O. BOX 208
BEDFORD, MA 01730
01CY ATTN JOHN MORGANSTERN
01CY ATTN G. HARDING
01CY ATTN C. E. CALLAHAN

MITRE CORP
WESTGATE RESEARCH PARK
1820 DOLLY MADISON BLVD
MCLEAN, VA 22101
01CY ATTN W. HALL
01CY ATTN W. FOSTER

PACIFIC-SIERRA RESEARCH CORP
1456 CLOVERFIELD BLVD.
SANTA MONICA, CA 90404
01CY ATTN E. C. FIELD JR

PENNSYLVANIA STATE UNIVERSITY
IONOSPHERE RESEARCH LAB
318 ELECTRICAL ENGINEERING EAST
UNIVERSITY PARK, PA 16802
(NO CLASSIFIED TO THIS ADDRESS)
01CY ATTN IONOSPHERIC RESEARCH LAB

PHOTOMETRICS, INC.
442 MARRETT ROAD
LEXINGTON, MA 02173
01CY ATTN IRVING L. KOFSKY

TECHNOLOGY INTERNATIONAL CORP
75 WIGGINS AVENUE
BEDFORD, MA 01730
01CY ATTN W. P. BOQUIST

TRW DEFENSE & SPACE SYS GROUP
ONE SPACE PARK
REDONDO BEACH, CA 90278
01CY ATTN R. K. PLEBUCH
01CY ATTN S. ALTSCHULER
01CY ATTN D. DEE

SRI INTERNATIONAL
333 RAVENSWOOD AVENUE
MENLO PARK, CA 94025
01CY ATTN DONALD NEILSON
01CY ATTN ALAN BURNS
01CY ATTN G. SMITH
01CY ATTN L. L. COBB
01CY ATTN DAVID A. JOHNSON
01CY ATTN WALTER G. CHESNUT
01CY ATTN CHARLES L. RINO
01CY ATTN WALTER JAYE
01CY ATTN M. BARON
01CY ATTN RAY L. LEADABRAND
01CY ATTN G. CARPENTER
01CY ATTN G. PRICE
01CY ATTN J. PETERSON
01CY ATTN R. HAKE, JR.
01CY ATTN V. GONZALES
01CY ATTN D. McDANIEL

IONOSPHERIC MODELING DISTRIBUTION LIST
UNCLASSIFIED ONLY

PLEASE DISTRIBUTE ONE COPY TO EACH OF THE FOLLOWING PEOPLE:

ADVANCED RESEARCH PROJECTS AGENCY
(ARPA)
STRATEGIC TECHNOLOGY OFFICE
ARLINGTON, VIRGINIA

CAPT. DONALD M. LEVINE

NAVAL RESEARCH LABORATORY
WASHINGTON, D.C. 20375

DR. P. MANGE
DR. R. MEIER
DR. E. SZUSZCZEWICZ - CODE 4127
DR. J. GOODMAN - CODE 7560

SCIENCE APPLICATIONS, INC.
1250 PROSPECT PLAZA
LA JOLLA, CALIFORNIA 92037

DR. D. A. HAMLIN
DR. L. LINSON
DR. D. SACHS

DIRECTOR OF SPACE AND ENVIRONMENTAL
LABORATORY NOAA
BOULDER, COLORADO 80302

DR. A. GLENN JEAN
DR. G. W. ADAMS
DR. D. N. ANDERSON
DR. K. DAVIES
DR. R. F. DONNELLY

A. F. GEOPHYSICS LABORATORY
L. G. HANSOM FIELD
BEDFORD, MASS. 01730

DR. T. ELKINS
DR. W. SWIDER
MRS. R. SAGALYN
DR. J. M. FORBES
DR. T. J. KENESHEA
DR. J. AARONS

OFFICE OF NAVAL RESEARCH
800 NORTH QUINCY STREET
ARLINGTON, VIRGINIA 22217

DR. H. MULLANEY

COMMANDER
NAVAL OCEAN SYSTEMS CENTER
SAN DIEGO, CALIFORNIA 92152

MR. R. ROSE - CODE 5321

U. S. ARMY ABERDEEN RESEARCH AND
DEVELOPMENT CENTER
BALLISTIC RESEARCH LABORATORY
ABERDEEN, MARYLAND

DR. J. HEIMERL

COMMANDER
NAVAL AIR SYSTEMS COMMAND
DEPARTMENT OF THE NAVY
WASHINGTON, D.C. 20360

DR. T. CZUBA

HARVARD UNIVERSITY
HARVARD SQUARE
CAMBRIDGE, MASS. 02138

DR. M. B. MCELROY
DR. R. LINDZEN

PENNSYLVANIA STATE UNIVERSITY
UNIVERSITY PARK, PENNSYLVANIA 16802

DR. J. S. NISBET
DR. P. R. ROHRBAUGH
DR. L. A. CARPENTER
DR. M. LEE
DR. R. DIVANY
DR. P. BENNETT
DR. F. KLEVANS

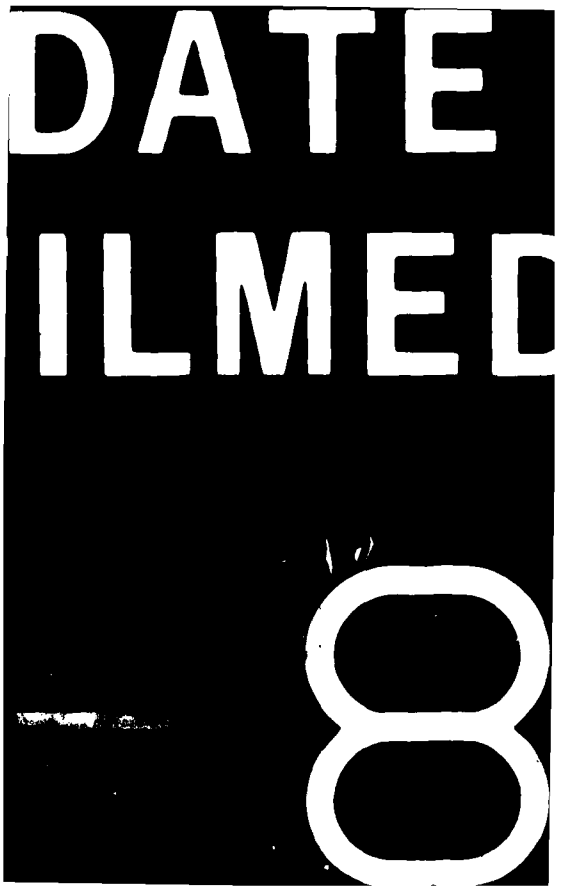
DATE
ILMED
8